

## A New Tool To Guide Halofunctionalization Reactions: The Halenium Affinity (*HalA*) Scale

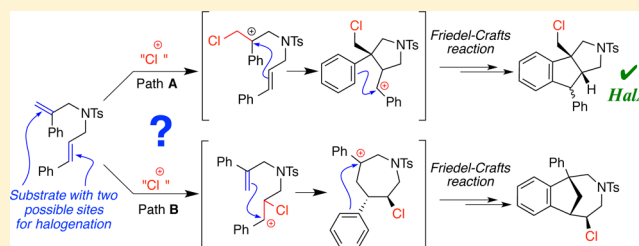
Kumar Dilip Ashtekar,<sup>†,‡</sup> Nastaran Salehi Marzijarani,<sup>†,‡</sup> Arvind Jaganathan,<sup>§</sup> Daniel Holmes,<sup>†</sup> James E. Jackson,<sup>\*,†</sup> and Babak Borhan<sup>\*,†</sup>

<sup>§</sup>Engineering and Process Sciences, The Dow Chemical Company, Midland, Michigan 48674, United States

<sup>†</sup>Department of Chemistry, Michigan State University, East Lansing, Michigan 48824, United States

### Supporting Information

**ABSTRACT:** We introduce a previously unexplored parameter—halenium affinity (*HalA*)—as a quantitative descriptor of the bond strengths of various functional groups to halenium ions. The *HalA* scale ranks potential halenium ion acceptors based on their ability to stabilize a “free halenium ion”. Alkenes in particular but other Lewis bases as well, such as amines, amides, carbonyls, and ether oxygen atoms, etc., have been classified on the *HalA* scale. This indirect approach enables a rapid and straightforward prediction of chemoselectivity for systems involved in halofunctionalization reactions that have multiple nucleophilic sites. The influences of subtle electronic and steric variations, as well as the less predictable anchimeric and stereoelectronic effects, are intrinsically accounted for by *HalA* computations, providing quantitative assessments beyond simple “chemical intuition”. This combined theoretical–experimental approach offers an expeditious means of predicting and identifying unprecedented reactions.



As a class, halenium ion donors<sup>1</sup> are electrophilic reagents that offer access to complex and useful molecular motifs.<sup>2</sup> Oxidation, addition to  $\pi$ -bonds, halogenation of aromatics, and activation of heteroatoms are among their core reaction modes. The electronegativity, bonding flexibility, and delivery reagents for halogen cations strongly modulate their selectivity. For instance, some chlolenium donors are effective alcohol oxidants,<sup>3</sup> whereas suitably chosen iodenium reagents achieve mild activations to form selected glycosidic bonds without oxidation of alcoholic functionalities.<sup>4</sup> The key to this diversity of reactivity lies in the variable interactions of halenium ions with different functional groups.

Electrophilic activation of alkenes via halenium ion attack has been extensively studied for its ability to forge C–C, C–O, C–N, and C–X bonds. The past decade has witnessed explosive growth, especially in the field of stereoselective halofunctionalization of alkenes.<sup>5</sup> Despite this rapid expansion and great synthetic utility, the field is still in its infancy and has yet to witness benchmarks analogous in generality and utility to asymmetric epoxidations, dihydroxylations, aminohydroxylations, hydrogenations, cyclopropanations, hydrometalations, oxidative cleavage, and aziridinations, among others.<sup>6</sup> Several studies have probed the mechanistic underpinnings of halenium ion reactions,<sup>5a,7</sup> but state of the art halofunctionalizations still rely on trial-and-error approaches to reaction discovery and development/optimization.

To expedite discovery of new reactions in this area, an organizing framework is needed. Reflecting on our own synthetic<sup>8</sup> and mechanistic<sup>9</sup> ventures, we note the parallels between protonation and halogenation of alkenes. The field

would be well served by a scale like the familiar  $pK_a$  tables, to classify and order the halenium ion affinities of various functional groups. Herein we present such a scale, computationally derived but validated by experiments, that quantitatively predicts not only the interactions of halenium ions with various Lewis base acceptors but also the processes that ensue after the capture of halenium ion by a substrate molecule.

We begin by addressing a question that is fundamental to all alkene halogenation reactions: How easily does a given alkene capture a halenium ion? More specifically, how can we *quantify* the propensity of an alkene to undergo halogenation using reliable and predictable means? We approached this question using theoretical means by comparing protonation and halogenation chemistry. While there is ample literature precedent for determination of *proton affinities*, an analogous approach with halenium ions (perhaps surprisingly) finds no such precedence. In analogy to *ab initio* derived proton affinities (*PA*),<sup>10</sup> we have developed a scale of *HalA* with the aid of experiments and theoretical calculations. We have developed the *HalA* scale with the aid of experiments and theoretical calculations. For a wide range of halenium acceptors, *HalA* serves as a ruler to predict the relative ease of electrophilic halogenation.

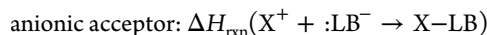
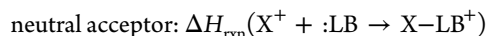
We define the *HalA* value for a given Lewis base (:LB) as the DFT<sup>11</sup> calculated energy change upon attachment of a halenium ion ( $X^+$ ). The B3LYP/6-31G\* theoretical method was chosen largely based on its popularity, low cost, wide

Received: July 12, 2014

Published: August 25, 2014

availability, and success in relation to our experimental studies. Likewise, the use of the SM8 solvation model<sup>11f,12</sup> and LANL2DZ pseudopotential<sup>11h</sup> and basis set for iodine were default but effective choices available in the Spartan<sup>11i</sup> software package.

The acceptor fragment may be neutral or anionic (i.e., the X–LB complex is cationic or neutral), leading to two distinct cases:



The *HalA* values in kcal/mol are derived at  $T = 298.15$  K (unless noted otherwise) as in eqs 1 and 2:

$$\text{HalA} = -\Delta E_{\text{(elec)}} - \Delta \text{ZPE} - \Delta E'_{\text{(vib)}} + \frac{5}{2}RT \quad (1)$$

$$E'_{\text{(vib)}}(T) = \sum_{i=1}^{3n-6} \frac{N h \nu_i}{e^{N h \nu_i / RT} - 1} \quad (2)$$

where  $\Delta E_{\text{(elec)}} = E_{\text{(electronic)}}(\text{X-LB adduct}) - [E_{\text{(electronic)}}(\text{:LB}) + E_{\text{(electronic)}}(\text{X}^+)]$ ; zero point energy change  $\Delta \text{ZPE} = \text{ZPE}(\text{X-LB adduct}) - \text{ZPE}(\text{:LB})$ ;  $\Delta E'_{\text{(vib)}} = E'_{\text{(vib)}}(\text{X-LB adduct}) - E'_{\text{(vib)}}(\text{:LB})$ , i.e., difference in temperature dependence of vibrational energy;  $N$  is Avogadro's number,  $h$  is Planck's constant, and  $\nu_i$  is the  $i^{\text{th}}$  vibrational frequency. Finally, the  $(5/2)RT$  quantity accounts for translational degrees of freedom and the ideal gas value for the change from two particles to one. The energy used for the free halonium ion is the value calculated for its (6-electron,  $s^2p^4$ ) triplet ground state.<sup>13</sup>

Table 1 shows an illustrative set of *HalA* values for styrenes, taken from this study's list of over 500 halonium acceptors with various functional groups (see Supporting Information); for reference, Table 1 lists absolute *HalA* values for styrene. As expected, for a given substrate, *HalA* drops with decreasing halogen electronegativity. Likewise, methyl substitution on

**Table 1. Theoretically Estimated Relative *HalA* (Gas Phase) and PA for Some Illustrative Styrylic Systems<sup>c</sup>**

Entry	Neutral Acceptors	<i>HalA</i> (X)				
		<i>HalA</i> <sup>a</sup> (F) kcal/mol	<i>HalA</i> <sup>a</sup> (Cl) kcal/mol	<i>HalA</i> <sup>a</sup> (Br) kcal/mol	<i>HalA</i> <sup>b</sup> (I) kcal/mol	<i>PA</i> <sup>a</sup> (H) kcal/mol
1		<b>0.0</b> (300.5)	<b>0.0</b> (167.4)	<b>0.0</b> (124.7)	<b>0.0</b> (94.1)	<b>0.0</b> (212.5)
2		9.6	6.7	5.2	4.2	5.7
3		2.8	2.2	1.4	0.3	-3.2
4		5.7	0.8	0.3	-0.4	-2.7

<sup>a</sup>B3LYP/6-31G\*. <sup>b</sup>B3LYP/6-31G\*/LANL2DZ. <sup>c</sup>Numbers in parentheses are absolute *HalA* and PA values for styrene in kcal/mol.

styrene (entries 2–4) increases *HalA* via stabilization of the haloalkylcarbenium ion. Though these variations are qualitatively predictable, the *HalA* computations place them on a quantitative basis. Interestingly, an insightful and counter-

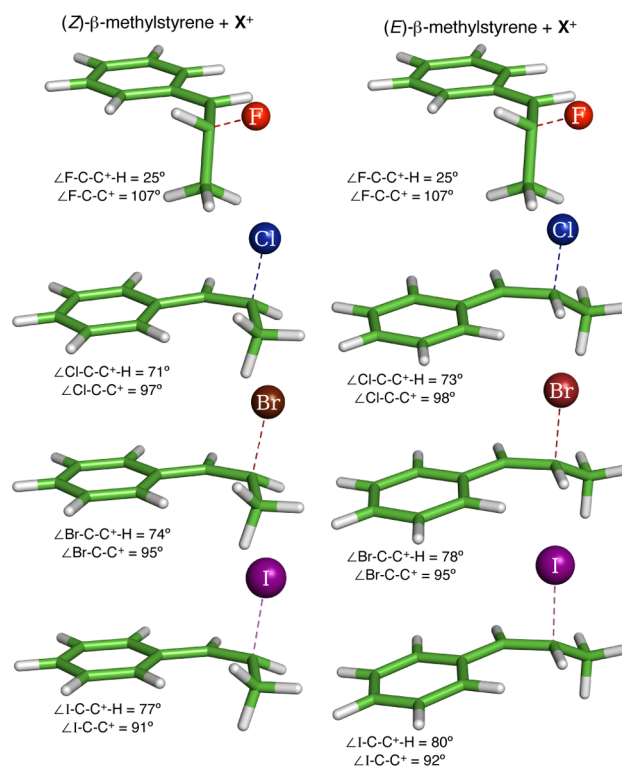
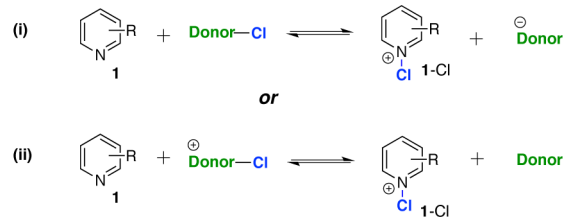


**Figure 1.** Geometry minimized structures of (*E*)- and (*Z*)- $\beta$ -methylstyrene upon treatment with different halonium ions. B3LYP/6-31G\* for *HalA* (F, Cl, and Br). B3LYP/6-31G\*/LANL2DZ for *HalA* (I).



Halonium Ion Acceptors	<i>HalA</i> (Cl) kcal/mol
	<b>0.0</b> (148.2)
	<b>32.9</b>
	<b>29.5</b>
	<b>20.1</b>
	<b>-0.1</b>

**Figure 2.** Theoretically estimated relative *HalA* values for pyridine **1a** in comparison to the counterions of commonly employed chloronium sources (B3LYP/6-31G\*/SM8 acetone).

intuitive result was obtained by comparison of *HalA* (F) of  $\beta$ -methylstyrenes (entries 3 and 4, Table 1). In agreement with reports by Sauer<sup>14</sup> and our previous findings for chloronium ion,<sup>9a</sup> the *HalA* predictions for bromonium and iodonium affinities of (*E*)- and (*Z*)- $\beta$ -methylstyrene also find an open carbocation minimum (see Figure 1). Evidence for this comes from the lengthened C(benzylic)–X bond distance computed for Br and I (as seen earlier for Cl), and a relatively short length for the C(homobenzylic)–X bond, which is close to the expected normal bond length for each system. Although the optimized structures do find the C–X bond aligned with the benzylic cation's empty 2p orbital, the <3.5 kcal/mol barrier to –C(CH<sub>3</sub>)HX rotation reflects no significant preference for

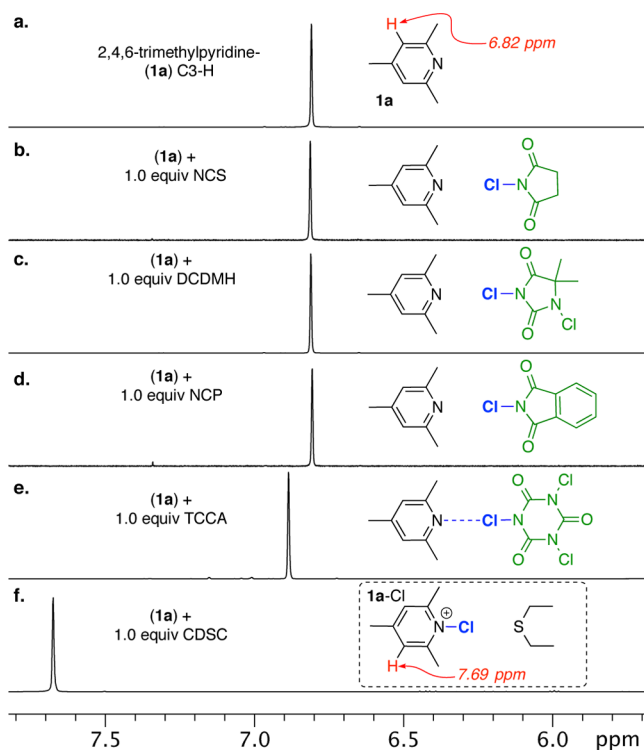


**Figure 3.** Overlay of  $^1\text{H}$  NMR (500 MHz, acetone- $d_6$ ) spectra (a–f). Spectrum a represents a section of  $^1\text{H}$  NMR displaying the C3-H of **1a**, whereas overlay of spectra b–f shows the effects of treatment of **1a** with different chloronium sources: NCS (*N*-chlorosuccinimide), DCDMH (1,3-dichloro-5,5-dimethylhydantoin), NCP (*N*-chlorophthalimide), TCCA (trichloroisocyanuric acid), CDSC (chlorodiethylsulfonium antimony(VI) chloride).

bridging.<sup>9a,14</sup> This result explains the higher *HalA* (Cl, Br, and I) values for the *E*-isomer as compared to its sterically congested *Z*-analogue (where such an alignment of C–X bond is skewed due to allylic strain).

As often occurs among halogens, fluorine is unique in its behavior. The *HalA* (F) computations for the  $\beta$ -methylstyrenes find affinities of 303.3 kcal/mol for the *E*-isomer and 306.2 kcal/mol for the *Z*-isomer ( $\Delta\text{HalA} = 2.9$  kcal/mol in favor of *Z*-isomer). A closer inspection of the minimized models reveals that, regardless of initial geometry, (*E*)- and (*Z*)- $\beta$ -methylstyrene gives the same 1-fluoromethyl-carbenium ion with the C–F bond orthogonal to the benzylic cation's empty 2p orbital. This stark difference reflects the reluctance of the C–F bond to donate into the adjacent empty 2p orbital (owing to the fluorine atom's high electronegativity), which in turn forces the C–C bond to be aligned with the empty orbital. Thus, the difference in *HalA* (F) values for *E*- and *Z*-isomers arises only from their differing allylic strain that is relieved upon formation of the common fluoromethyl carbenium ion intermediate.<sup>15</sup> As the halogens' electronegativity decreases from F to I, the tendency of the C–X bond to align with the empty 2p orbital rises as shown by the calculated ( $\angle\text{X}-\text{C}-\text{C}^+$ ) bond angles. Thus, though the charge (+1) is the same for each intermediate, the *HalA* analyses of these four styrenic acceptors serve to highlight the variations among the interaction modes of halonium ions.

Comparing halonium ions as electrophiles suggests reference to the most familiar electrophile: the proton. Is *HalA* simply a rehash of the familiar proton affinity (PA) scale? Clearly not.

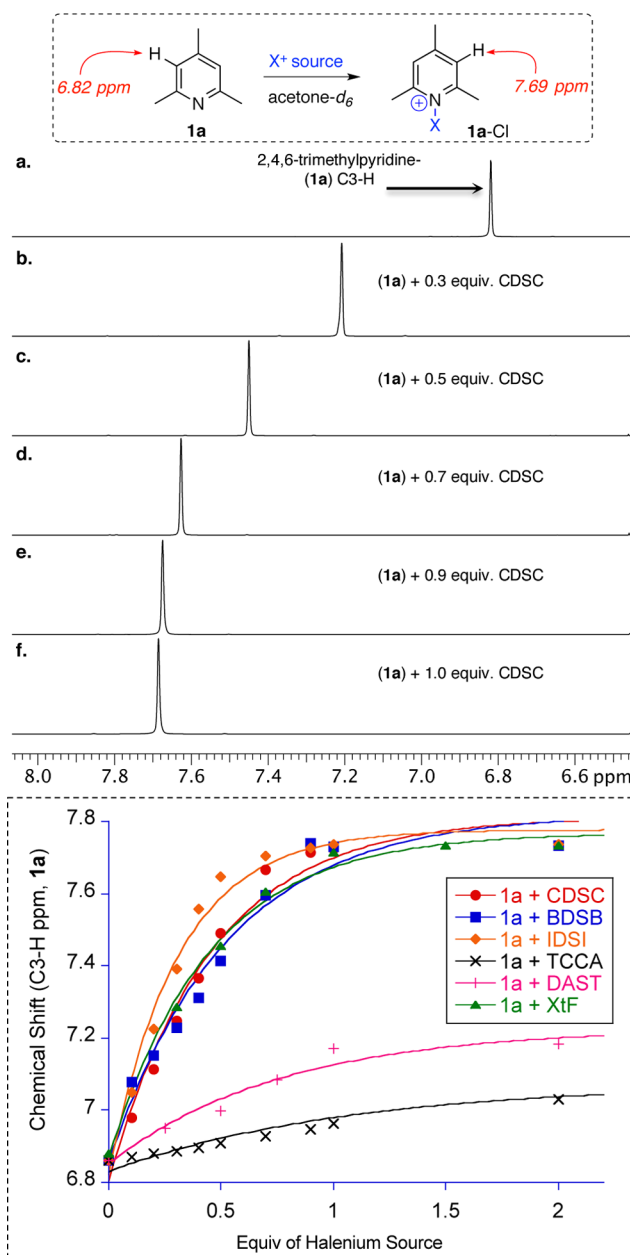


**Figure 4.** Spectra a–f depicts  $^1\text{H}$  NMR data for titration of **1a** with CDSC. The plot below shows change in chemical shift of C3-H of **1a** upon titration with different halonium sources. CDSC (chlorodiethylsulfonium antimony(VI) chloride), BDSB (bromodiethylsulfonium antimony(VI) halide), IDSI (iododiethylsulfonium antimony(VI) halide), XtF (Xtalfluor-E).

Very different conformational preferences are seen for analogous acceptor–proton vs acceptor–halonium ion complexes, with the energetic orderings even inverted in some cases. For instance, as seen in Table 1, and earlier pointed out by Kafafi and Liebman,<sup>16</sup> the (*E*) and (*Z*) analogues of  $\beta$ -methylstyrene (entries 3 and 4) have lower *PA* values than styrene itself. Evidently, the stabilizing electron donation by the  $\beta$ -methyl groups is more significant in the starting olefin than in

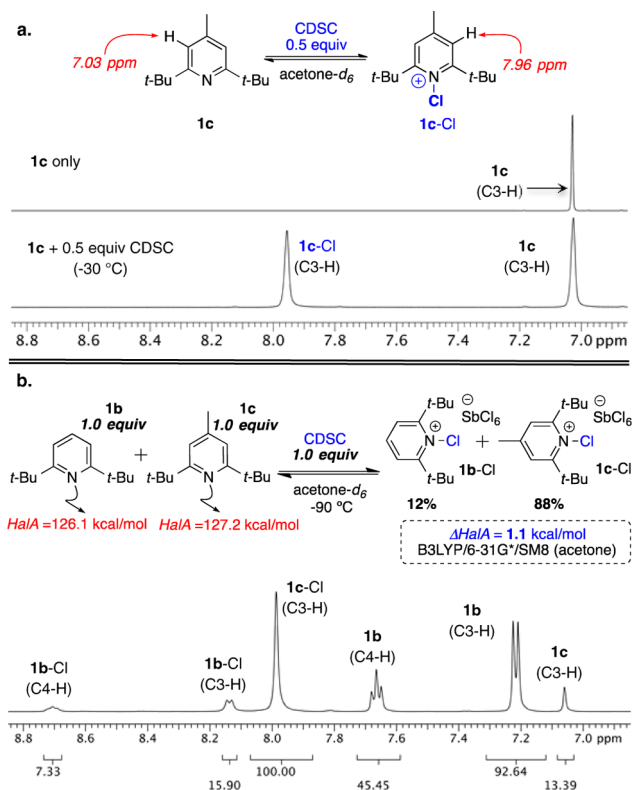


**Figure 5.** (a) Partial chlorination of **1c** using 0.5 equiv of CDSC leads to distinctly observable species **1c** and **1c-Cl** at  $-30\text{ }^{\circ}\text{C}$  by  $^1\text{H}$  NMR (500 MHz). (b) Competition study between **1b** and **1c** in acetone- $d_6$  at  $-90\text{ }^{\circ}\text{C}$  as quantified by  $^1\text{H}$  NMR.

the cation formed by proton capture. In contrast, all three methylstyrene isomers show higher *HalA* values than the parent styrene. Thus, the *PA* scale is distinct from *HalA*. Furthermore, as Table 1 shows, significant differences are seen among the halogens, due to variations in their size, electronegativity, and polarizability. More *HalA* trends based on ring strain, orbital overlap contributions, donation effects, and other secondary interactions are shown in the Supporting Information (S6–S11).

In order to determine how well experimental results agree with the theoretically predicted *HalA* values, we initiated studies on *N*-halopyridinium salts, simple systems where halonium affinity can be easily quantified via  $^1\text{H}$  NMR. These salts have been well characterized and reported as potent halonium sources. The corresponding bromonium and iodonium salts are stable even at room temperature,<sup>17</sup> and the chloronium analogues, though unstable to isolation, have been characterized and observed via ESI studies.<sup>18</sup> Substituted pyridines (**1**) were chosen as halonium acceptors for preliminary  $^1\text{H}$  NMR studies (see Figure 2). Treatment of **1** (acceptor) with chloronium sources ( $\text{Cl}^+$  donors) forms the chloropyridinium ion (**1-Cl**) with expulsion of the donor counterion. For such a transfer of halonium ion to ensue, the *HalA* ( $\text{Cl}$ ) of **1** should be higher than that of the corresponding donor counterion.

Figure 2 depicts the theoretical *HalA* ( $\text{Cl}$ ) values for counterions of commonly employed chloronium sources in comparison to **1a**. Based on these estimates, the equilibrium for reaction (i) should favor the reactant side as the anions **A–C** have a significantly higher *HalA* than **1a**. Furthermore, based on the calculated *HalA* for the least nucleophilic anion **D**, the

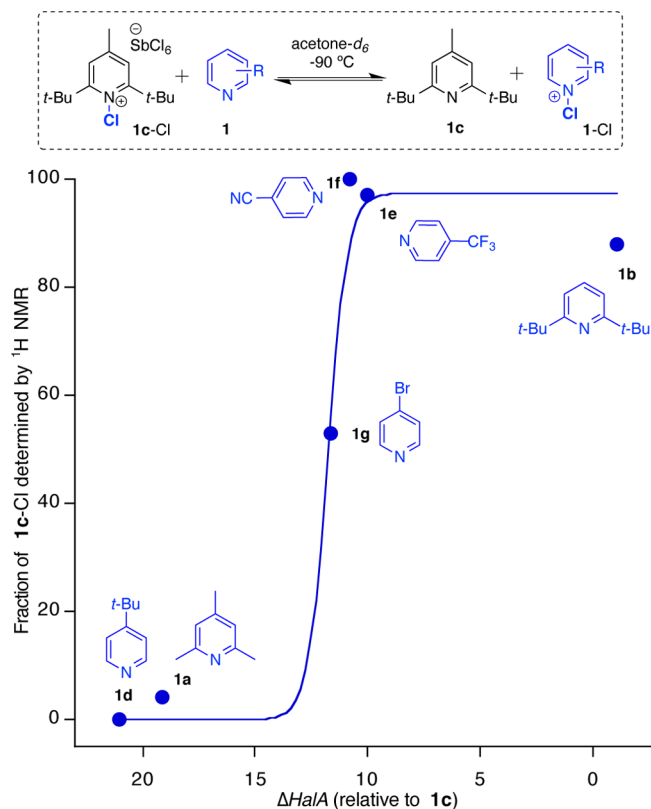


**Figure 6.** Comparison of  $\Delta\text{HalA}$  ( $\text{Cl}$ ) (B3LYP/6-31G\*/SM8) with experimental results of equilibrium studies between **1c-Cl** (prepared in situ using 1.0 equiv of CDSC) in the presence of 1.0 equiv of pyridines **1b–g**. The sigmoidal curve fit ( $R^2 = 0.974$ ) is derived from the Henderson–Hasselbalch equation.

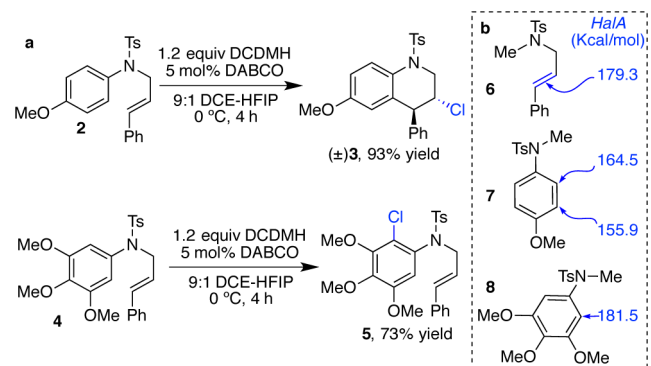


**Figure 7.** (a) Example of two reactions under identical conditions with different chemoselectivity. (b) *HalA* ( $\text{Cl}$ ) values (B3LYP/6-31G\*) for the reactive components of **2** and **4**.

chloronium ion is probably shared (but not completely transferred) between **1a** and anion **D**. To verify these predictions, **1a** was treated with the corresponding halonium sources and the interactions were assessed via the downfield  $^1\text{H}$  NMR shift of the C3-H resonance.

As a reference point to assess the extent of halonium ion transfer, we referred to the observed chemical shift difference between the free base-**1a** (C3-H at 6.82 ppm) and its protonated salt **1a-H**<sup>19</sup> (C3-H at 7.66 ppm) in acetone- $d_6$  ( $\Delta\text{ppm} = 0.84$ ) at room temperature. As with the protonation, to ensure the formation of **1a-Cl**, chlorodiethylsulfonium antimony(V) hexachloride (CDSC)<sup>20</sup> proved to be the most



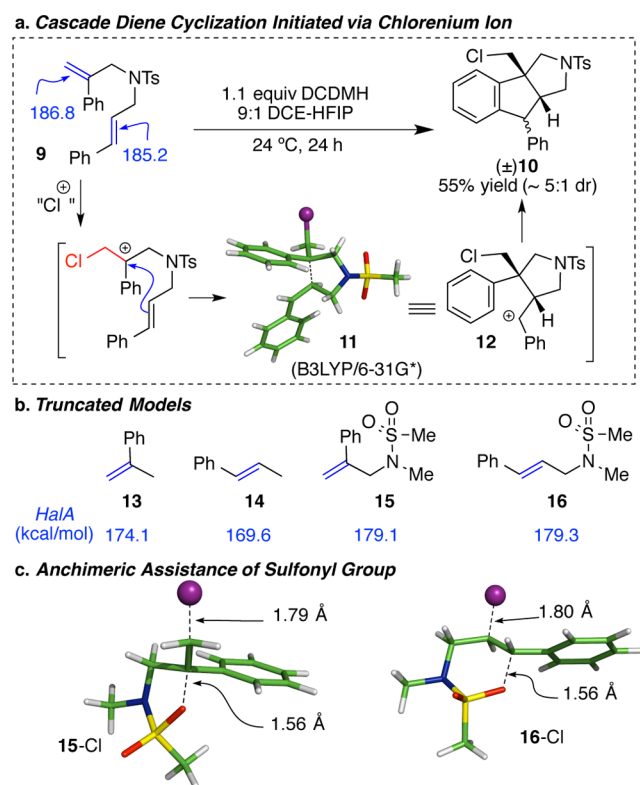


**Figure 8.** (a) Chlorocyclization of diene **9** to **10** is predicted by the higher *HalA* (Cl) of the 1,1-disubstituted olefin. Intermediate **11** is the computationally assessed outcome upon geometry minimization of **9** with chlorenium ion (B3LYP/6-31G\*). (b) *HalA* (Cl) values for the reactive components in the cyclization of **9**, illustrating the effect of *N*-Me substitution. (c) Anchimeric assistance of the sulfonyl group toward stabilization of the chlorocarbenium ion **15-Cl** and **16-Cl** as predicted by *HalA* calculations.

effective chlorenium ion source. The resulting chloropyridinium **1a-Cl** displayed a downfield shift of C3-H at 7.69 ppm ( $\Delta\text{ppm} = 0.87$ ). Figure 3 shows the experimental  $^1\text{H}$  NMR spectra of **1a** upon treatment with stoichiometric amounts of different chlorenium ion sources (spectra b–f). Spectra b–d clearly show that pyridine **1a** with a *HalA* (Cl) = 148.2 kcal/mol is incapable of abstracting a chlorenium ion from commonly employed imide based chlorenium donors (such as NCS, DCDMH, and NCP) whose counterions have higher *HalA*(Cl) values (i.e., >148.2 kcal/mol). Even TCCA, the most potent chlorenium source among the imide based chlorenium donors, results in only a 0.1 ppm downfield shift of C3-H of **1a** indicating halogen bonding (tight van der Waals complex) rather than complete chlorenium ion transfer (see spectrum e).<sup>21</sup> These experimental results compliment the theoretical *HalA* predictions.

Since reaction of neutral species to form ionic products would always be energetically uphill in organic solvent, transfer of chlorenium ion to **1a** calls for the use of a cationic chlorenium reagent (see reaction (ii), Figure 2). With this aim, CDSC, whose conjugate leaving group has a lower *HalA* (Cl) value (161.3 kcal/mol, gas phase) than **1a**, was employed.<sup>22</sup> Addition of 1.0 equiv of this reagent to **1a** effects the formation of **1a-Cl** as indicated by the 0.9 ppm downfield shift of C3-H (spectrum f), after a complete transfer of the chlorenium ion.<sup>23</sup>

Apart from **1a**, several substituted pyridines with varying electronic and steric profiles were subjected to similar analysis

using fluorenyl, chlorenium, bromenium, and iodenium sources to further evaluate *HalA* estimations (see Supporting Information). In all these cases the formation of a 1:1 complex of Lewis base:halenium ion was confirmed via  $^1\text{H}$  NMR analysis; the chemical shift of C3-H of **1a-Cl** (spectrum f) remained unchanged upon addition of superstoichiometric quantities of halenium source (see plot in Figure 4, dashed box).

To rigorously validate *HalA* assessments on a quantitative scale, we resorted to equilibrium studies of chloropyridinium salts. Quantitative *HalA* determination via  $^1\text{H}$  NMR analyses was complicated by the tendency of *N*-halopyridinium ion **1a-Cl** to undergo dimerization<sup>24</sup> with the free base **1a** when subjected to substoichiometric amounts of halenium source.<sup>17a</sup> Treatment of **1a** with 0.5 equiv of BDSB (or IDSI) in  $\text{CDCl}_3$  displayed a downfield shift of C3-H to 7.2 ppm. The extent of this shift is in accordance with the reported halogenated dimers of **1a**.<sup>17d</sup> Figure 4 displays the plot for the observed  $^1\text{H}$  NMR chemical shift (average of **1a** and **1a-X**) for C3-H when **1a** was titrated with different halenium sources (see plot). As seen from the overlay of  $^1\text{H}$  NMR spectra a–f (Figure 4), due to rapid exchange and possible dimerization, **1a** and **1a-Cl** could not be observed as individual species on the NMR time scale. To overcome this limitation, pyridines **1b** and **1c** were used for equilibrium studies of 1:1 complexes with CDSC as a chlorenium source. The bulky *t*-butyl substituents in the ortho positions efficiently inhibit the dimerization as well as rapid intermolecular transfer of halenium ions. As a consequence, the chlorinated pyridinium (**1c-Cl**) and the free base (**1c**) were observed as distinct species at  $-30$  °C via  $^1\text{H}$  NMR under substoichiometric amounts of the halogenating reagent (see Figure 5a).

Figure 5b displays a competition experiment between the two pyridines **1b** and **1c**, which have similar electronic and steric profiles. As anticipated, the gas phase *HalA* values predict **1c** to have a slightly increased Lewis basicity as a result of the 4-Me substituent ( $\Delta\text{HalA} = 2.6$  kcal/mol). For a better quantitative representation, an SM8 model<sup>12</sup> for simulated acetone was applied which attenuated the difference in their *HalA* values to 1.1 kcal/mol (Figure 5b). When an equimolar mixture of **1b** and **1c** was treated with 1.0 equiv of CDSC, an equilibrium mixture of **1c-Cl** and **1b-Cl** in  $\sim 7:1$  ratio was observed by  $^1\text{H}$  NMR. The experimental result is in good agreement with the theoretical *HalA* predictions ( $\Delta\text{HalA} = 1.1$  kcal/mol; predicting a 7:1 ratio). This study not only validates quantification via *HalA* but also signifies its importance in reliably predicting the outcome of reactions involving subtle steric and electronic changes.

In NMR studies of equilibria/competitions for halenium ions between pyridine **1b** and a series of substituted pyridines (**1a–g**, Figure 6), the trend of relative halenium affinities (theoretical) was found to parallel the equilibrium ratios of the competing Lewis bases (experimental), as elucidated by  $^1\text{H}$  NMR.

To explore the practical use of *HalA*, we applied it as a mechanistic tool to predict the stereo-, regio-, and chemo-selectivity of electrophilic alkene halogenations. The following examples were chosen for proof-of-principle studies. As shown in Figure 7, a Friedel–Crafts reaction of electron rich arenes is initiated via chlorenium ion activation of a pendant alkene. Substrate **2** with a 4-MeO- $\text{C}_6\text{H}_4$  substituent cleanly affords the desired cyclized product ( $\pm$ )-**3** upon treatment with DCDMH (Figure 7a). Under identical conditions, substrate **4** with the

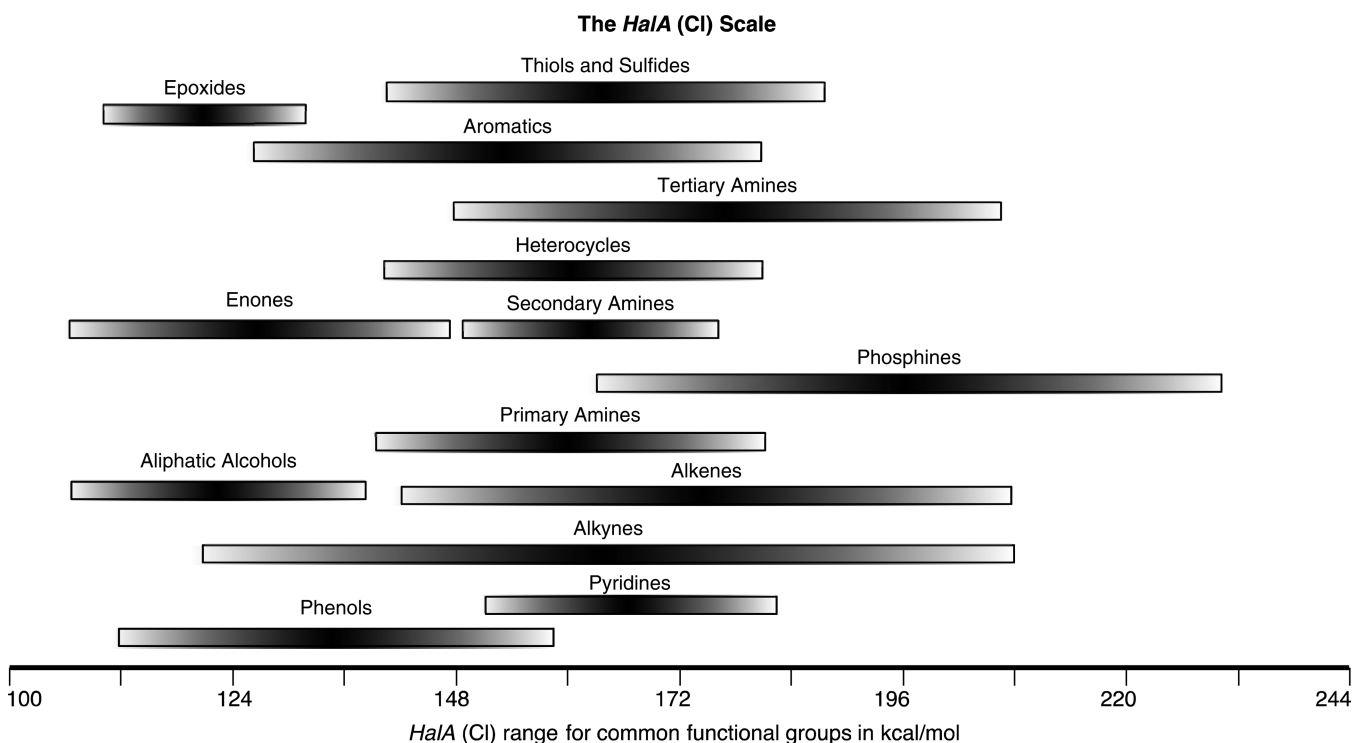


**Figure 9.** *HalA* (Cl) scale based on theoretical estimates of over 500 chlorine ion acceptors evaluated at the B3LYP/6-31G\* (gas phase) level of theory.

significantly more electron rich aromatic ring undergoes exclusively electrophilic aromatic substitution yielding product **5**. This chemoselectivity is readily predicted by *HalA* values. The nucleophilic aryl carbon of substrate **2** is predicted to have  $\sim 14$  kcal/mol lower halonium affinity than the olefin (*HalA* values were calculated on truncated systems, see **6** vs **7**, Figure 7b). The aryl ring of **4** on the other hand has about 2.2 kcal/mol higher halonium affinity than the olefin (see **6** vs **8**, Figure 7b) despite the steric demand associated with the formation of the pentasubstituted aryl core of **5**. Hence, the observed chemoselectivity may not be easily predicted or quantified. The *HalA* values additionally serve to quantify this selectivity and thereby enable such predictions with a greater level of confidence.

The next reaction represents an example where chemoselectivity prediction (either qualitative or quantitative) may be much less intuitive, with guesswork easily leading to the incorrect prediction. The treatment of diene **9** with a chlorine source affords **10** as the major product (Figure 8a).<sup>25</sup> The chlorination of the 1,1-disubstituted olefin followed by a nucleophilic attack on the resulting chlorocarbenium ion by the *trans*-olefin is necessary for the formation of the observed product. The *HalA* (Cl) values for  $\alpha$ - and  $\beta$ -methylstyrene (**13** and **14**) reveal a 4.5 kcal/mol higher halonium affinity for  $\alpha$ -methylstyrene (capable of forming a 3° carbenium). Interestingly, inclusion of the electron withdrawing *N*-sulfonyl group to better represent the structure of diene **9** greatly attenuates the difference in *HalA* values for the truncated structures **15** and **16** ( $\Delta HalA = 0.2$  kcal/mol). Notably, the counterintuitive increase in individual *HalA* (Cl) values with the introduction of the *N*-methyl sulfonamide results from anchimeric assistance of the neighboring sulfonamide that overrides any inductively deactivating effects (Figure 8c). The S–O bond of the *N*-sulfonyl group assists the

stabilization of the chloromethyl carbenium ion generated from  $\alpha$ - and  $\beta$ -methylstyrene. This extended delocalization (*internal solvation*) in the cationic intermediates **15**-Cl and **16**-Cl is responsible for the higher halonium affinity of **15** and **16** over **13** and **14**, which lack the *N*-sulfonyl tether (also see Figure 1). From a practical viewpoint, this small difference suggests negligible selectivity between the two olefinic moieties in these “truncated” models. However, a detailed Boltzmann gated conformational search of the diene substrate **9** (for calculations, the *N*-Ms variant was employed instead of *N*-Ts), followed by *HalA* evaluation for the lowest energy conformers of the two possible chlorocarbenium ions, predicts the experimental outcome to be favored by 1.6 kcal/mol over chlorination of the *trans*- $\beta$ -methyl styryl moiety. Moreover, the anchimeric assistance of the olefinic moiety of *trans*- $\beta$ -methyl styryl substituent, as shown in intermediate **11** (Figure 8a), is energetically preferred over the anchimeric assistance of the S–O bond from the *N*-Ms group by 2.3 kcal/mol. This example underscores the utility of the *HalA* method for the accurate prediction of chemoselectivity in alkene halogenation reactions. The experimental confirmation of the theoretically predicted chemoselectivity suggests that even small energetic preferences ( $\leq 2$  kcal/mol) can be reliably distinguished with *HalA* values.

Qualitative reactivity ranking of potential halogen attack sites using *HalA* computations can be made using the *HalA* table (Supporting Information) whereas quantitative comparison of affinities can be established by computing the full structures using appropriate solvation models. Figure 9 provides the *HalA* (Cl) scale for various functional groups to allow a qualitative comparison. As shown in Figure 9, functional groups (acceptors) that feature extended conjugation with the substituents attached span a larger range of *HalA*. For instance, alkenes, alkynes, amines, aromatic compounds, etc., whose HOMO can be easily perturbed by their substituents, display a

wider range of *HalA* values in comparison to epoxides or alcohols where the attached substituents can only exert a weaker inductive effect. A comparison of halonium affinities can (a) facilitate rational selection of compatible nucleophiles (especially when the nucleophilic atom is embedded within motifs that have similar steric/electronic profiles); (b) account for the modulation of *HalA* values of alkenes by the anchimeric assistance of neighboring functionalities (this aspect underscores the importance of quantitatively evaluating *HalA* values on full structures rather than on truncated models; furthermore, subtle electronic perturbations leading to modulations of *HalA* values are also accounted for in the calculations); and (c) accurately predict chemoselectivity, aiding in the development of halonium initiated cascade/Domino reactions.

These studies highlight the *HalA* scale's use as a design/predictive tool in a field heretofore dependent on trial-and-error approaches for reaction discovery. Like the  $pK_a$  scale, *halonium affinity* is a thermodynamic quantity and may not work to predict kinetically determined reaction outcomes. For such problems, more complete structural and energetic analyses of reaction paths and transition states<sup>26</sup> would be necessary.

The scope of "affinity tools", such as *HalA*, that broadly predict reaction chemoselectivities is certainly not limited exclusively to alkene halogenation reactions. Any electrophilic species (such as sulfenium, selenium, oxenium ions) capable of activating Lewis basic functionalities (such as olefins, alkynes, allenes, amines, etc.) can be efficiently parametrized on a similar scale to expedite the development of electrophilic functionalization reactions in general. These studies are ongoing and will be the subject of future disclosures.

## ■ ASSOCIATED CONTENT

### 📄 Supporting Information

Experimental details, *HalA* calculations, characterization data, DFT computational data, and MS Office Excel template for *HalA* calculations. This material is available free of charge via the Internet at <http://pubs.acs.org>.

## ■ AUTHOR INFORMATION

### Corresponding Authors

\*babak@chemistry.msu.edu

\*jackson@chemistry.msu.edu

### Author Contributions

‡These authors contributed equally.

### Notes

The authors declare no competing financial interest.

## ■ ACKNOWLEDGMENTS

Generous support was provided in part by the NIH (GM110525) and the NSF (CHE-1362812). The authors acknowledge the help of Edward Toma, Christopher Rahn, Aaron Schmidt, Thomas Chen, Ashley Burkin, and Meghan Richardson (undergraduate collaborators). We are indebted to Professor Daniel Jones (MSU) for his guidance on matters of mass spectrometry.

## ■ REFERENCES

(1) (a) Bose, A.; Mal, P. *Tetrahedron Lett.* **2014**, *55*, 2154. (b) Chen, J.; Zhou, L. *Synthesis* **2014**, *46*, 586. (c) de Mattos, M. C. S. *Curr. Org. Synth.* **2013**, *10*, 819. (d) Galligan, M. J.; Akula, R.; Ibrahim, H. *Org. Lett.* **2014**, *16*, 600. (e) Getrey, L.; Krieg, T.; Hollmann, F.; Schrader, J.; Holtmann, D. *Green Chem.* **2014**, *16*, 1104. (f) Kamei, T.; Ishibashi, A.; Shimada, T. *Tetrahedron Lett.* **2014**, *55*, 4245. (g) Stodulski, M.;

Goetzinger, A.; Kohlhepp, S. V.; Gulder, T. *Chem. Commun.* **2014**, *50*, 3435.

(2) (a) Murphy, C. D. *J. Appl. Microbiol.* **2003**, *94*, 539. (b) Neumann, C. S.; Fujimori, D. G.; Walsh, C. T. *Chem. Biol.* **2008**, *15*, 99.

(3) (a) Hiegel, G. A.; Nalbandy, M. *Synth. Commun.* **1992**, *22*, 1589. (b) van Summeren, R. P.; Romaniuk, A.; Ijpeij, E. G.; Alsters, P. L. *Catal. Sci. Technol.* **2012**, *2*, 2052.

(4) (a) Hasty, S. J.; Demchenko, A. V. *Chem. Heterocycl. Compd.* **2012**, *48*, 220. (b) Girard, N.; Rousseau, C.; Martin, O. R. *Tetrahedron Lett.* **2003**, *44*, 8971. (c) Fraser-Reid, B.; Lopez, C. J.; Gammon, D. W.; Sels, B. F. In *Handbook of Chemical Glycosylation: Advances in Stereoselectivity and Therapeutic Relevance*; Demchenko, A. V., Ed.; Wiley: 2008; p 381.

(5) (a) In *Halogen Bonding: Fundamentals and Applications*; Metrangolo, P., Resnati, G., Eds.; Springer-Verlag Berlin: Berlin, 2008; Vol. 126, p 1. (b) Chen, G.; Ma, S. *Angew. Chem., Int. Ed.* **2010**, *49*, 8306. (c) Castellanos, A.; Fletcher, S. P. *Chem.—Eur. J.* **2011**, *17*, 5766. (d) Denmark, S. E.; Kuester, W. E.; Burk, M. T. *Angew. Chem., Int. Ed.* **2012**, *51*, 10938. (e) Hennecke, U. *Chem.—Asian J.* **2012**, *7*, 456. (f) Mendoza, A.; Fanas, F. J.; Rodriguez, F. *Curr. Org. Synth.* **2013**, *10*, 384. (g) Murai, K.; Fujioka, H. *Heterocycles* **2013**, *87*, 763. (h) Tan, C. K.; Yeung, Y.-Y. *Chem. Commun.* **2013**, *49*, 7985. (i) Chen, J.; Zhou, L. *Synthesis* **2014**, *46*, 586. (j) Zheng, S.; Schienebeck, C. M.; Zhang, W.; Wang, H.-Y.; Tang, W. *Asian J. Org. Chem.* **2014**, *3*, 366.

(6) (a) Ojima, I. *Catalytic asymmetric synthesis*, 2nd ed.; Wiley-VCH: New York, 2000. (b) Sweeney, J. B. *Chem. Soc. Rev.* **2002**, *31*, 247.

(7) (a) Denmark, S. E.; Burk, M. T.; Hoover, A. J. *J. Am. Chem. Soc.* **2010**, *132*, 1232. (b) McManus, S. P.; Peterson, P. E. *Tetrahedron Lett.* **1975**, 2753. (c) Ohta, B. K.; Hough, R. E.; Schubert, J. W. *Org. Lett.* **2007**, *9*, 2317. (d) Olah, G. A.; Bolling, J. M. *J. Am. Chem. Soc.* **1968**, *90*, 947. (e) Olah, G. A.; Bolling, J. M.; Brinich, J. J. *J. Am. Chem. Soc.* **1968**, *90*, 6988. (f) Olah, G. A.; Peterson, P. E. *J. Am. Chem. Soc.* **1968**, *90*, 4675. (g) Olah, G. A.; Westerman, P. W.; Melby, E. G.; Mo, Y. K. *J. Am. Chem. Soc.* **1974**, *96*, 3565. (h) Solling, T. I.; Radom, L. *Int. J. Mass Spectrom.* **1999**, *185*, 263.

(8) (a) Garzan, A.; Jaganathan, A.; Marzizarani, N. S.; Yousefi, R.; Whitehead, D. C.; Jackson, J. E.; Borhan, B. *Chem.—Eur. J.* **2013**, *19*, 9015. (b) Jaganathan, A.; Garzan, A.; Whitehead, D. C.; Staples, R. J.; Borhan, B. *Angew. Chem., Int. Ed.* **2011**, *50*, 2593. (c) Jaganathan, A.; Staples, R. J.; Borhan, B. *J. Am. Chem. Soc.* **2013**, *135*, 14806. (d) Whitehead, D. C.; Fhaner, M.; Borhan, B. *Tetrahedron Lett.* **2011**, *52*, 2288. (e) Whitehead, D. C.; Yousefi, R.; Jaganathan, A.; Borhan, B. *J. Am. Chem. Soc.* **2010**, *132*, 3298.

(9) (a) Yousefi, R.; Ashtekar, K. D.; Whitehead, D. C.; Jackson, J. E.; Borhan, B. *J. Am. Chem. Soc.* **2013**, *135*, 14524. (b) Yousefi, R.; Whitehead, D. C.; Mueller, J. M.; Staples, R. J.; Borhan, B. *Org. Lett.* **2011**, *13*, 608.

(10) (a) Curtiss, L. A.; Raghavachari, K.; Pople, J. A. *J. Chem. Phys.* **1993**, *98*, 1293. (b) Delbene, J. E. *J. Phys. Chem.* **1993**, *97*, 107. (c) Smith, B. J.; Radom, L. *J. Am. Chem. Soc.* **1993**, *115*, 4885.

(11) (a) Becke, A. D. *J. Chem. Phys.* **1993**, *98*, 5648. (b) Becke, A. D. *J. Chem. Phys.* **1993**, *98*, 1372. (c) Becke, A. D. *J. Chem. Phys.* **1993**, *98*, 5648. (d) Hariharan, P. C.; Pople, J. A. *Theor. Chim. Acta* **1973**, *28*, 213. (e) Hehre, W. J.; Ditchfield, R.; Pople, J. A. *J. Chem. Phys.* **1972**, *56*, 2257. (f) Marenich, A. V.; Olson, R. M.; Kelly, C. P.; Cramer, C. J.; Truhlar, D. G. *J. Chem. Theory Comput.* **2007**, *3*, 2011. (g) Stephens, P. J.; Devlin, F. J.; Chabalowski, C. F.; Frisch, M. J. *J. Phys. Chem.* **1994**, *98*, 11623. (h) Wadt, W. R.; Hay, P. J. *J. Chem. Phys.* **1985**, *82*, 284. (i) Spartan '10. Wavefunction, Inc.: Irvine, CA, 2010.

(12) Cramer, C. J.; Truhlar, D. G. *Rev. Comput. Chem.* **1995**, *1*.

(13) Li, Y.; Wang, X.; Jensen, F.; Houk, K. N.; Olah, G. A. *J. Am. Chem. Soc.* **1990**, *112*, 3922.

(14) Haubenstock, H.; Sauers, R. R. *Tetrahedron* **2005**, *61*, 8358.

(15) The geometry minimized structures of (*E*)- and (*Z*)- $\beta$ -methyl styrene at the B3LYP/6-31G\* level of theory finds a 2.9 kcal/mol higher energy for the *Z*-isomer.

(16) Kafafi, S. A.; Mautner, M.; Liebman, J. F. *Struct. Chem.* **1990**, *1*, 101.

(17) (a) Baruah, S. K.; Baruah, R. *Asian J. Chem.* **2004**, *16*, 688. (b) Haque, I.; Wood, J. L. *J. Mol. Struct.* **1968**, *2*, 217. (c) Homsy, F.; Rousseau, G. *J. Org. Chem.* **1999**, *64*, 81. (d) Homsy, F.; Sylvie, R.; Rousseau, G. *Org. Synth.* **2000**, *77*, 206. (e) Kleinberg, J. *J. Chem. Educ.* **1946**, *23*, 559. (f) Mendes, C.; Renard, S.; Rofoo, M.; Roux, M. C.; Rousseau, G. *Eur. J. Org. Chem.* **2003**, 463. (g) Zingaro, R. A.; Goodrich, J. E.; Kleinberg, J.; Vanderwerf, C. A. *J. Am. Chem. Soc.* **1949**, *71*, 575. (h) Zingaro, R. A.; Tolberg, W. E. *J. Am. Chem. Soc.* **1959**, *81*, 1353.

(18) Gozzo, F. C.; Eberlin, M. N. *J. Mass Spectrom.* **2001**, *36*, 1140.

(19) For a fair comparison between the protonated and chlorinated pyridiniums, the same counteranion,  $\text{SbCl}_6^-$ , was employed.

(20) Snyder, S. A.; Treitler, D. S.; Brucks, A. P. *J. Am. Chem. Soc.* **2010**, *132*, 14303.

(21) It is noteworthy that 1.0 equiv of TCCA accounts for 3.0 equiv of active chlorgenium ion. This NMR experiment was performed in the dark using acetone- $d_6$  purged with  $\text{O}_2$  gas prior to TCCA addition, to avoid radical chlorination. Along with the described complex, products of benzylic chlorination (most likely via radical pathway) were observed by NMR when the same experiment was performed with the reaction mixture being exposed to light and open to atmosphere.

(22) B3LYP/6-31G\*/SM8 is not compatible for the antimony(VI) chloride counterion associated with CDSC. Hence we resorted to comparison of gas phase *HalA* (Cl) values of diethyl sulfide and **1a**. The gas phase *HalA* (Cl) value of **1a** is 168.2 kcal/mol whereas diethyl sulfide has a *HalA* value of 161.3 kcal/mol.

(23) (a) We recognize the possibility that treatment of pyridines with halenium sources in acetone as a solvent might lead to protonation (rather than chlorination) of the pyridinium nitrogen atom yielding  $\alpha$ -chloroacetone as a byproduct. This possibility was ruled out based on the following control experiments: (1) no change in chemical shift of the chloropyridiniums upon addition of  $\text{K}_2\text{CO}_3$ ; (2) employing THF as a solvent to observe similar resonances of C3-H of the free base **1a** and its chlorinated counterpart **1a-Cl**; and (3) employing the in situ generated chloropyridinium **1a-Cl** toward successfully initiating a chlorolactonization of 4-phenylpent-4-enoic acid (see Supporting Information for experimental details). (b) Gil, V. M. S.; Murrell, J. N. *Trans. Faraday Soc.* **1964**, *60*, 248.

(24) Karim, A.; Reitti, M.; Carlsson, A.-C. C.; Grafenstein, J.; Erdelyi, M. *Chem. Sci.* **2014**, *5*, 3226.

(25) Crude  $^1\text{H}$  NMR analysis indicated a 5:1 dr for **10**. Although complete conversion of **9** was attained as judged by TLC and  $^1\text{H}$  NMR, the mass balance was accounted by a complex mixture of products, which were inseparable by chromatography. Identity of these products could not be assigned due to overlapping peaks in NMR. An analytically pure sample of **10** was obtained via preparative TLC.

(26) Crehuet, R.; Bofill, J. M. *J. Chem. Phys.* **2005**, 122.